doi: 10.15407/ujpe62.07.0557

V.A. KOVALCHUK,[1,2] A.YU. KORCHIN [1,2]

[1] NSC "Kharkiv Institute of Physics and Technology", NAS of Ukraine
(Akademichna, 1, 61108 Kharkiv, Ukraine)
[2] V.N. Karazin Kharkiv National University
(Svobody Sq., 4, 61022 Kharkiv, Ukraine; e-mail: koval@kipt.kharkov.ua)

PACS 11.30.Er, 14.80.Cp

HIGGS BOSON DECAY TO LEPTON PAIR AND PHOTON AND POSSIBLE NON-HERMITICITY OF THE YUKAWA INTERACTION

The production of lepton pairs in the Higgs boson decay $h \to \ell^+\ell^-\gamma$ is studied. The emphasis is put on the structure of the Higgs boson interaction with fermions. This interaction is chosen as a mixture of the scalar and pseudo-scalar couplings, and, in addition, it is supposed to be non-Hermitian. We study predictions of this model for the observables in the $h \to \ell^+\ell^-\gamma$ decay for e^+e^-, $\mu^+\mu^-$, and $\tau^+\tau^-$ pairs. The differential decay width and lepton forward-backward asymmetry are calculated as functions of the dilepton invariant mass for several sets of $hf\bar{f}$ coupling constants. The influence of the non-Hermitian $hf\bar{f}$ interaction on the forward-backward asymmetry is studied, and the large influence of a possible non-Hermiticity of the Higgs interaction with the top quarks on the forward-backward asymmetry for e^+e^- and $\mu^+\mu^-$ pairs is stressed.

Keywords: Higgs boson, non-Hermitian interaction, decay of a Higgs boson.

1. Introduction

In 2012, the collaborations ATLAS and CMS at the Large Hadron Collider (LHC) discovered the spin-less particle h with the mass about 125 GeV [1, 2]. The study of the processes of production of the h boson and its decay channels allowed one to conclude [3, 4] that its characteristics are consistent with properties of the Higgs boson of the Standard model (SM). In particular, the analysis of the angular correlations in the decays $h \to ZZ^*$, $Z\gamma^*$, $\gamma^*\gamma^* \to 4\ell$, $h \to WW^* \to \ell\nu\ell\nu$ ($\ell = e, \mu$), and $h \to \gamma\gamma$ revealed that all the data agree with predictions for the Higgs boson with the quantum numbers $J^{\rm PC} = 0^{++}$ [5–7].

The masses of the fermions in the SM arise due to the Yukawa interaction between the Higgs field and the fermion fields. The investigation of this interaction is necessary for the identification of the particle h with the Higgs boson of the SM. Particularly, it is important to check whether the Higgs boson interaction with fermions is Hermitian or not. Moreover, it is necessary also to verify the Hermiticity of the Yukawa interaction Lagrangian [8].

Presently for the decay modes $h \to \tau^+\tau^-$ and $h \to b\bar{b}$, the Higgs signal strength parameter $\mu(X)$ is determined. This is the ratio of the experimentally measured cross-section of the Higgs boson production with the subsequent decay into a certain final state X to the corresponding value calculated in the SM:

$$\mu(X) = \frac{\sigma(pp \to h)_{\rm exp}{\rm BR}(h \to X)_{\rm exp}}{\sigma(pp \to h)_{\rm SM}{\rm BR}(h \to X)_{\rm SM}}. \quad (1)$$

There are ATLAS and CMS measurements of the production cross-section and decay rate of the Higgs boson, as well as the constraints on the coupling constants of the interaction with vector bosons and fermions. The result of this analysis is the values $\mu(\tau^+\tau^-) = 1.12 \pm 0.23$ and $\mu(b\bar{b}) = 0.82 \pm 0.30$ [9].

Some aspects of a possible non-Hermiticity of the Higgs boson interaction with the top-quark have been studied in [10–12]. Namely, in [10, 11], the polarization characteristics of the photon in the decay processes $h \to \gamma\gamma$ and $h \to \gamma Z$ were studied. The photon circular polarization in these decays arises due to the presence of the $\mathcal{CP}$-even and $\mathcal{CP}$-odd components in the $ht\bar{t}$ interaction, small imaginary loop contribution in the SM, and non-Hermiticity of the $ht\bar{t}$ interaction. In [12], it was shown that the lepton forward-backward asymmetry A_{FB} in the processes $h \to \gamma\ell^+\ell^-$ (for $\ell = e, \mu, \tau$) is sensitive to a possible non-Hermiticity of the Higgs interaction with the top-quark. We emphasize that the measurement of any observable, which is sensitive to a non-Hermiticity of the Lagrangian, can be used at the same time for testing the $\mathcal{CPT}$ theorem, since the Hermiticity of the Hamiltonian (or Lagrangian) is the necessary condition in the proof of the $\mathcal{CPT}$ theorem in quantum field theory (see, e.g., [13]).

In the present paper, we consider the influence of a possible non-Hermiticity of the Higgs boson interaction with fermions (leptons and quarks), which contains both scalar and pseudoscalar parts, on the decay $h \to \gamma\ell^+\ell^-$, where $\ell = (e,\, \mu,\, \tau)$. We calculate the differential decay rate and lepton forward-backward asymmetry as functions of the invariant mass of the lepton pair, and discuss the decay rate integrated over invariant masses and the asymmetry.

2. Decay Amplitudes and Angular Distribution

We assume that the interaction of the h-boson with the fermion fields, ψ_f, is described by the Lagrangian

$$\mathcal{L}_{hff} = -\sum_{f=\ell,\, q} \frac{m_f}{v}\, h\, \bar{\psi}_f\, (a_f + i\, b_f \gamma_5)\, \psi_f, \qquad (2)$$

which includes both scalar and pseudoscalar parts.

Here, $v = (\sqrt{2} G_F)^{-1/2} \approx 246$ GeV is the vacuum expectation value of the Higgs filed, $G_F = 1.1663787(6) \times 10^{-5}$ GeV^{-2} is the Fermi constant [9], m_f is the fermion mass, and a_f and b_f are complex-valued parameters (of course, $a_f = 1$ and $b_f = 0$ correspond to the SM). One can consider (2) as a phenomenological parametrization of effects of "new physics" (NP) beyond the SM. At the same time, the interaction with the $W^\pm$ and Z bosons is taken as in the SM. For real values of parameters a_f and b_f, interaction (2) is Hermitian. However, it is straightforward to verify [8] that the width of the h-boson decay to the fermion pair in the lowest order is the same for Hermitian and non-Hermitian Lagrangians (2).

We consider the h-boson decay

$$h(p) \to \gamma(k,\, \epsilon(k)) + \ell^+(q_+) + \ell^-(q_-), \qquad (3)$$

where the 4-momenta of the h boson, photon, and leptons are, respectively, p, k, q_+, q_-, and $\epsilon(k)$ is the 4-vector of the photon polarization.

The differential decay width can be written as

$$\frac{\mathrm{d}\Gamma}{\mathrm{d}q^2\, \mathrm{d}\cos\theta} = \frac{\beta_\ell (m_h^2 - q^2)}{(8\pi)^3\, m_h^3} \sum_{\text{pol}} |\mathcal{M}|^2, \qquad (4)$$

where m_h is the mass of the h boson, $q \equiv q_+ + q_-$, q^2 is the invariant mass squared of the lepton pair, $\beta_\ell = \sqrt{1 - 4m_\ell^2/q^2}$ is the velocity of a lepton in the rest frame of the lepton pair. The polar angle θ is determined in this frame; it is the angle between the momentum of the l^+ lepton and the axis, which is opposite to the direction of motion of the Higgs boson.

The decay amplitude is

$$\mathcal{M} = \mathcal{M}_{\text{tree}} + \mathcal{M}_{\text{loop}}, \qquad (5)$$

where the tree-level amplitude (see Fig. 1) is

$$\mathcal{M}_{\text{tree}} = c_0\, \epsilon_\mu^*(k)\, \bar{u}(q_-)(a_\ell + i\, b_\ell \gamma_5) \times \times \left(\frac{2q_+^\mu + \not{k}\gamma^\mu}{2k\cdot q_+} - \frac{2q_-^\mu + \gamma^\mu \not{k}}{2k\cdot q_-} \right) v(q_+), \qquad (6)$$

with

$$c_0 = e m_\ell Q_\ell\, (\sqrt{2} G_F)^{1/2}, \qquad (7)$$

$e = \sqrt{4\pi\alpha_{G_F}}$ is the electric charge of a positron, $Q_\ell = -1$ (lepton charge in units of e), and m_ℓ is the lepton mass. The electromagnetic coupling constant in the G_F scheme [14] is $\alpha_{G_F} = \sqrt{2} G_F m_W^2 (1 - m_W^2/m_Z^2)/\pi$, where $m_W (m_Z)$ is the mass of the $W(Z)$ boson.

The one-loop contributions to the $h \to \gamma\, \gamma^*/Z^* \to \gamma\ell^+\ell^-$ decay (see Fig. 1) can be written in the form

$$\mathcal{M}_{\text{loop}} = \epsilon_\mu^*(k)[(q^\mu k^\nu - g^{\mu\nu} kq) \times \times \bar{u}(q_-)(c_1\gamma_\nu + c_2\gamma_\nu\gamma_5) v(q_+) - - \epsilon^{\mu\nu\alpha\beta} k_\alpha q_\beta\, \bar{u}(q_-)(c_3\gamma_\nu + c_4\gamma_\nu\gamma_5) v(q_+)], \qquad (8)$$

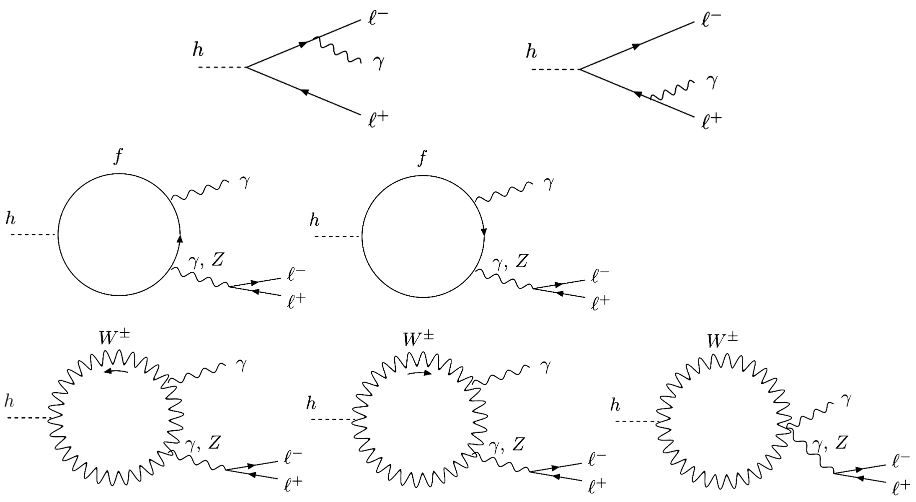

Fig. 1. Diagrams of the process $h \to \gamma \ell^+ \ell^-$: the tree-level diagrams are shown on the top, one-loop diagrams – on the bottom. Fermions f are denoted by solid lines, gauge bosons $W^\pm, Z, \gamma$ – by wavy lines, and the h boson – by dashed lines

with the coefficients $c_1, ..., c_4$, which have been obtained in [12] and are collected for convenience in Appendix A. In addition, $\epsilon_{0123} = +1$.

In the present work, we do not include the box-type loop contributions to the process $h \to \gamma \ell^+ \ell^-$. The contribution from these diagrams in the SM is very small [15, 16]. In addition, there are other mechanisms, $h \to \gamma V \to \gamma \ell^+ \ell^-$, where V is an intermediate vector resonance decaying to the $\ell^+ \ell^-$ pair, which can contribute to the decay $h \to \gamma \ell^+ \ell^-$. Particularly, the production of charmonium $J/\psi\,(c\bar{c})$ and bottomonium $\Upsilon(1S)\,(b\bar{b})$ is of interest for studying the $hq\bar{q}$ interaction (see, e.g., [17–20]). However, these processes lie beyond the scope of the present work.

Calculating amplitude (5) squared and summed over the polarizations of leptons and a photon in model (2), we obtain

$$\sum_{\text{pol}} |\mathcal{M}|^2 = c_0^2 \left[|a_\ell|^2 A + |b_\ell|^2 \widetilde{A} \right] + \\ + 2c_0 \big[\text{Re}(c_1\, a_\ell^*) B + \text{Im}(c_2\, b_\ell^*) \widetilde{B} + \\ + \text{Im}(c_4\, a_\ell^*) C + \text{Re}(c_3\, b_\ell^*) \widetilde{C} \big] + \\ + \big(|c_1|^2 + |c_3|^2\big) D + \big(|c_2|^2 + |c_4|^2\big) E + \\ + 2\text{Im}\big(c_1 c_4^* + c_2 c_3^*\big) F, \tag{9}$$

where A, $\widetilde{A}$, B, $\widetilde{B}$, C, $\widetilde{C}$, D, E, F have the same form as in [12] and are given in Appendix A.

The forward-backward (FB) asymmetry is defined (see, e.g., [12]) as

$$A_{\text{FB}}(q^2) = \left(\frac{d\Gamma_{\text{F}}}{dq^2} - \frac{d\Gamma_B}{dq^2} \right) \left(\frac{d\Gamma_F}{dq^2} + \frac{d\Gamma_B}{dq^2} \right)^{-1}, \tag{10}$$

where

$$\frac{d\Gamma_F}{dq^2} \equiv \int_0^1 \frac{d\Gamma}{dq^2\, d\cos\theta}\, d\cos\theta, \\ \frac{d\Gamma_B}{dq^2} \equiv \int_{-1}^0 \frac{d\Gamma}{dq^2\, d\cos\theta}\, d\cos\theta, \tag{11}$$

and the q^2 integrated FB asymmetry reads

$$\langle A_{\text{FB}} \rangle = \left\langle \frac{d\Gamma_F}{dq^2} - \frac{d\Gamma_B}{dq^2} \right\rangle \Big/ \left\langle \frac{d\Gamma_F}{dq^2} + \frac{d\Gamma_B}{dq^2} \right\rangle, \tag{12}$$

with the notation

$$\langle J \rangle \equiv \int_{q^2_{\min}}^{q^2_{\max}} dq^2 J(q^2) \tag{13}$$

for the integration limits $q^2_{\min} \geq 4m_\ell^2$ and $q^2_{\max} \leq m_h^2$.

In Eqs. (9), only the coefficients $\widetilde{B}$, C, and F are linear in $\cos\theta$. Therefore, as can be seen from (4), (9), and (10), the numerator of the FB asymmetry (10) is determined by the imaginary combination of the terms $c_2\, b_\ell^* + c_4\, a_\ell^*$ and $c_1\, c_4^* + c_2\, c_3^*$:

$$\frac{d\Gamma_F}{dq^2} - \frac{d\Gamma_B}{dq^2} = -\frac{2(m_h^2 - q^2)^2}{(8\pi)^3\, m_h^3} \times \times \left[8m_\ell\, c_0 \mathrm{Im}(c_2\, b_\ell^* + c_4\, a_\ell^*) \ln\left(\frac{q^2}{4m_\ell^2}\right) + + \mathrm{Im}\,(c_1 c_4^* + c_2 c_3^*)\,(q^2 - 4m_\ell^2)\,(m_h^2 - q^2) \right]. \qquad (14)$$

In framework of the SM, the differential decay width (4), (9) takes a simpler form. In this case, $a_\ell = 1$, $b_\ell = 0$ and $c_{3,\,\mathrm{SM}} = c_{4,\,\mathrm{SM}} = 0$. Thus, the FB asymmetry vanishes,

$$A_{\mathrm{FB}}(q^2)_{\mathrm{SM}} = 0. \qquad (15)$$

Therefore, nonzero values of this asymmetry can arise only in certain models of new physics.

3. Results of Calculations and Discussion

First, we discuss the choice of the parameters a_f and b_f that determine the interaction of the Higgs boson with fermions (2). In the leading order, the rate of the h-boson decay to fermions, except the top quarks, has the form

$$\Gamma(h \to f\bar{f}) = \frac{N_f G_F}{4\sqrt{2}\pi} m_f^2 m_h \beta_f \left(|a_f|^2 \beta_f^2 + |b_f|^2\right), \quad (16)$$

where $\beta_f = \sqrt{1 - 4m_f^2/m_h^2}$ is the fermion velocity in the rest frame of h, $N_f = 1\,(3)$ for leptons (quarks). Apparently, β_f is equal to one with a good accuracy. We assume further that the $h \to f\bar{f}$ decay rate in model (2) is the same as in the SM, i.e.,

$$|a_f|^2 + |b_f|^2 = 1. \qquad (17)$$

In this case, to search for effects of new physics in the decay $h \to f\bar{f}$, it will be necessary to measure the polarization characteristics of the fermions, which clearly complicates the identification of the particle h with the Higgs boson of the SM.

Let us calculate the predictions of model (2) with the constraint $|a_f|^2 + |b_f|^2 = 1$ for the decay $h \to \gamma\ell^+\ell^-$ and check how much these predictions differ from the SM.

In the calculations, we use the parameters of NP presented in Table 1.

The new physics model NP1 is described by the parameters $a_f = 1/\sqrt{2}$, $b_f = 1/\sqrt{2}$ for all fermions, except the top quark, for which the couplings are taken from [21]. In the NP1 model, interaction (2) is Hermitian.

In the model NP2, $a_f = 1/\sqrt{2}$, $b_f = i/\sqrt{2}$. While we choose $a_t = 1.20$, $b_t = 0.37\,i$ for the top quark, so that interaction (2) becomes non-Hermitian. Finally, in the model NP3, the interaction for the leptons is non-Hermitian, while interaction (2) for all quarks is taken as in the SM.

The numerical values of other parameters of the SM are taken from [9], in particular, the masses of the $W^\pm$ and Z bosons, and the decay widths and couplings for $Zf\bar{f}$ interaction. The quark masses are chosen as in [14, 22], and $\sin^2\theta_W = 1 - m_W^2/m_Z^2$.

In Fig. 2, we present the differential width of the $h \to \ell^+\ell^-\gamma$ decay for various leptons $l = (e, \mu, \tau)$ calculated in the SM and in model (2) with the couplings in Table 1. The minimal photon energy in the rest frame of the h boson is chosen $E_\gamma^{\min} = 1$ GeV to cut off the infrared divergence at $E_\gamma \to 0$. This leads to the maximal value of the dilepton invariant mass $q_{\max} = (m_h^2 - 2m_h E_\gamma^{\min})^{1/2} \approx m_h - E_\gamma^{\min} = 124$ GeV for $m_h = 125.09$ GeV.

As one can see from Fig. 2, there are deviations from the SM predictions with the chosen parameters a_f, b_f. In Table 2, we also show the decay widths integrated over the invariant mass within the limits $[q_{\min}, q_{\max}]$.

In the interval of invariant masses from 1.0 GeV to 124.0 GeV, the effect of new physics does not exceed 5% in the decays $h \to \gamma e^+e^-$ and $h \to \gamma\mu^+\mu^-$. However, at small invariant masses below 30 GeV, this

Table 1. **Parameters of the $hf\bar{f}$ interaction in the SM and in several models of NP. Here, ℓ denotes leptons, and q denotes quarks of all flavors, except the top quark, for which parameters are shown separately**

$hf\bar{f}$ couplings	SM	NP1	NP2	NP3
a_ℓ	1	$\frac{1}{\sqrt{2}}$	$\frac{1}{\sqrt{2}}$	$\frac{1}{\sqrt{2}}$
b_ℓ	0	$\frac{1}{\sqrt{2}}$	$\frac{i}{\sqrt{2}}$	$\frac{i}{\sqrt{2}}$
a_q	1	$\frac{1}{\sqrt{2}}$	$\frac{1}{\sqrt{2}}$	1
b_q	0	$\frac{1}{\sqrt{2}}$	$\frac{i}{\sqrt{2}}$	0
a_t	1	1.2	1.2	1
b_t	0	0.37	$0.37i$	0

 ISSN 2071-0186. Ukr. J. Phys. 2017. Vol. 62, No. 7

effect reaches 10%, although the decay rate in this interval is very small as compared, for example, with the rate of the Higgs boson decay to two photons $\Gamma(h \to \gamma\gamma) = 9.28$ keV [14].

In Fig. 3, we show the forward-backward asymmetry (10). As was previously mentioned, the FB asymmetry takes zero value in the SM, and non-zero values can arise only in models beyond the SM. Of course, not all models of NP lead to non-zero FB asymmetry.

In Table 3, we also present the integrated FB asymmetry (12).

As is seen from Fig. 3, the FB asymmetry for the e^+e^- and $\mu^+\mu^-$ pairs for the real parameters a_f and b_f is very small, of the order of 1%. Only for the pair of the τ-leptons, this asymmetry reaches 2.5% at the invariant mass near the Z-boson mass.

The FB asymmetry for the e^+e^- and $\mu^+\mu^-$ pairs increases considerably for the non-Hermitian $hf\bar{f}$ interaction in the model NP2. Namely, the FB asymmetry can reach 15% for an electron-positron pair and 10% for a muon-antimuon pair. In the model NP3, in which only the interaction $h\ell^+\ell^-$ is non-Hermitian, the FB asymmetry is still very small. Thus, the most important contribution comes from the non-Hermiticity of the Higgs boson interaction with

Table 2. **The width of the decay $\Gamma(h \to \gamma\ell^+\ell^-)$ (in keV) for various lepton pairs in the invariant mass limits $[q_{min}, q_{max}]$ (in GeV)**

$\ell^+\ell^-$	q_{min}	q_{max}	SM	NP1	NP2	NP3
e^+e^-	1.0	124.0	0.34	0.32	0.32	0.34
	1.0	30.0	0.11	0.10	0.10	0.11
	37.5	75.0	0.02	0.02	0.02	0.02
$\mu^+\mu^-$	1.0	124.0	0.53	0.52	0.52	0.53
	1.0	30.0	0.11	0.10	0.10	0.11
	37.5	75.0	0.03	0.03	0.03	0.03
$\tau^+\tau^-$	4.0	124.0	31.0	31.1	31.1	31.1
	12.5	75.0	1.77	1.80	1.80	1.79

Table 3. **Forward-backward asymmetry in the decay $\Gamma(h \to \gamma\ell^+\ell^-)$ in % for various leptons in the limits of the invariant dilepton mass from q_{min} to q_{max} (in GeV)**

$\ell^+\ell^-$	q_{min}	q_{max}	NP1	NP2	NP3
e^+e^-	1.0	124.0	−0.36	0.78	−0.01
	1.0	30.0	0.01	0.61	−0.01
	37.5	75.0	−0.28	13.1	−0.1
$\mu^+\mu^-$	1.0	124.0	−0.24	0.52	0.03
	1.0	30.0	0.01	0.62	0.01
	37.5	75.0	−0.19	8.5	0.28
$\tau^+\tau^-$	4.0	124.0	−0.06	0.08	0.07
	12.5	75.0	−0.05	1.0	0.88

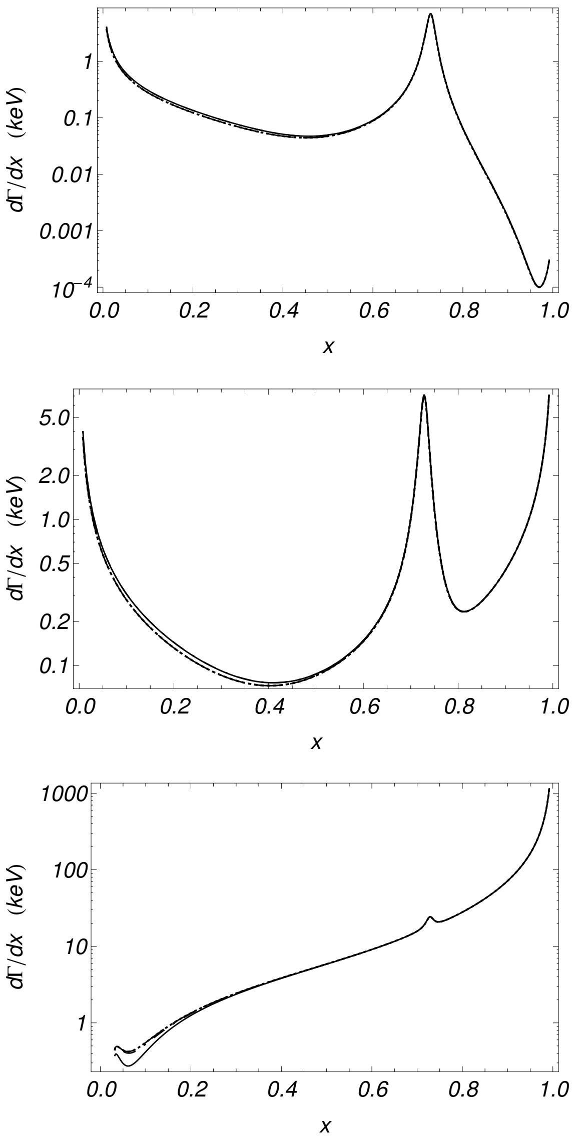

Fig. 2. Differential decay width of $h \to \gamma\ell^+\ell^-$ for various lepton pairs as a function of x, where $x \equiv \sqrt{q^2}/m_h$. The top part is drawn for the e^+e^- pair, the middle part – $\mu^+\mu^-$ pair, and the bottom part – $\tau^+\tau^-$ pair. The solid lines correspond to the SM, dotted lines – model NP1, dashed lines – model NP2, dash-dotted lines – model NP3

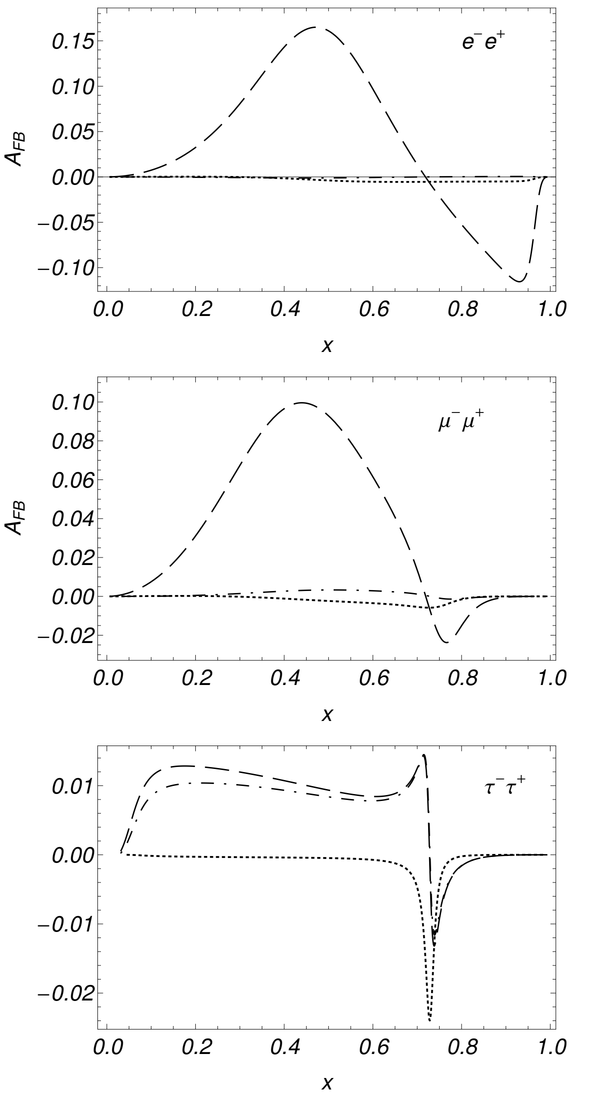

Fig. 3. Forward-backward asymmetry in the decay $h \to \to \gamma\ell^+\ell^-$ for various lepton pairs as a function of x, where $x \equiv \sqrt{q^2}/m_h$. The dotted lines correspond to NP1, dashed lines – NP2, dash-dotted lines – NP3

quarks, mainly with the top-quark. This $ht\bar{t}$ interaction enters the loop diagrams in Fig. 1.

As for the $\tau^+\tau^-$ pair, the behavior is different from the case of light leptons. In the process $h \to \tau^+\tau^-\gamma$, the dominant contribution comes from the tree-level diagram in Fig. 1. Therefore, the structure of the interaction of the Higgs boson with the tau lepton is crucial. This explains the observed tendency in Fig. 3, in which models NP2 and NP3 give the close results, though the absolute value of the FB asymmetry does not exceed 1.5%.

It is seen from Fig. 3 that the FB asymmetries change sign as functions of the variable $x = \sqrt{q^2}/m_h$. Therefore, the integration of the asymmetries over the whole interval of invariant masses gives small values. This is demonstrated in Table 3: the obtained values for the e^+e^- and $\mu^+\mu^-$ pairs are less than 1%, and, for the $\tau^+\tau^-$ pair, are less than 0.1%. However, choosing the suitable intervals of integration increases the corresponding values to 13.1% for the e^+e^- pair and to 8.5% for the $\mu^+\mu^-$ pair. For the $\tau^+\tau^-$ pair, the integrated FB asymmetry does not exceed 1%.

4. Conclusions

We studied the decay of the Higgs boson to a photon and a lepton-antilepton pair, i.e., $h \to \gamma\ell^+\ell^-$, where $\ell = (e, \mu, \tau)$. The differential decay width and the lepton forward-backward asymmetry are calculated as functions of the dilepton invariant mass.

These observables are calculated in the Standard model and in the model, in which the Higgs boson interaction with the fermions consists of scalar and pseudoscalar terms, which imply the CP violation. Moreover, we assume a possible non-Hermiticity of this interaction. The tree-level amplitudes and the one-loop $h \to \gamma Z^* \to \gamma\ell^+\ell^-$ and $h \to \gamma\gamma^* \to \gamma\ell^+\ell^-$ diagrams are included. The main emphasis is put on studying the effects of a possible non-Hermiticity of the $hf\bar{f}$ interaction on the observables.

The observables are calculated with the model parameters a_f, b_f chosen in such a way that the $h \to f\bar{f}$ decay rate (where $f = (\ell, q)$) coincides with the rate in the SM. For the couplings with the top quark, a_t, b_t, we choose the values from Ref. [21], which are constrained from all available data.

The calculations show that the differential decay widths for $h \to \gamma e^+e^-$ and $h \to \gamma\mu^+\mu^-$ are not very sensitive to effects of NP. Only at small values of the dilepton invariant mass below 30 GeV, the corrections to the SM prediction reach 10%, though the decay rate in this interval is rather small, about 0.1 keV.

The lepton forward-backward asymmetry $A_{\rm FB}$ is more sensitive to effects of NP, because this observable vanishes identically in the SM. However, for real parameters of the $hf\bar{f}$ interaction, $A_{\rm FB}$ is small, of the order of 1% for the e^+e^- and $\mu^+\mu^-$ pairs and 2.5% for the $\tau^+\tau^-$ pair. This asymmetry becomes sizable for the complex parameters a_f, b_f, i.e., for the non-Hermitian interaction. In particular, for the e^+e^- and $\mu^+\mu^-$ pairs, $A_{\rm FB}$ rises to 15% for the e^+e^- pair and to 10% for the $\mu^+\mu^-$ pair. The main contribution to $A_{\rm FB}$ comes from the non-Hermitian interaction of the Higgs boson with the top quark in the loop diagrams.

At the same time, for the $\tau^+\tau^-$ pair, the tree-level diagrams are dominant, and, thus, the asymmetry depends on the Higgs interaction with the tau leptons. It turns out that the effect of a non-Hermiticity in $A_{\rm FB}$ is of the order of 1%, which may be difficult for experimental studies.

Our consideration of the decays $h \to \gamma\ell^+\ell^-$ demonstrates that a possible non-Hermiticity of the $ht\bar{t}$ interaction has a big impact on the forward-backward asymmetry for the light leptons. The non-Hermiticity of the $h\ell^+\ell^-$ interaction does not show up in this observable. In summary, the forward-backward asymmetry in the $h \to \gamma e^+e^-$ and $h \to \gamma\mu^+\mu^-$ decays is the informative important observable for experimental studies at the LHC in the search for effects of new physics.

This research was partially supported by the Ministry of Education and Science of Ukraine (projects Nos. 0115U000473 and 0117U004866) and the National Academy of Sciences of Ukraine (project TsO-1-4/2016).

APPENDIX A
Definition of coefficients $c_1, ..., c_4$ and A, $\widetilde{A}$, B, $\widetilde{B}$, C, $\widetilde{C}$, D, E, F

In this Appendix, we present the coefficients $c_1, ..., c_4$ in Eq. (8), which are determined from the loop diagrams in Fig. 1. They read [12]

$$\begin{aligned} c_1 &= \frac{1}{2}\,\frac{g_{V,\ell}}{q^2 - m_Z^2 + im_Z\Gamma_Z}\,\Pi_Z + \frac{Q_\ell}{q^2}\,\Pi_\gamma, \\ c_2 &= -\frac{1}{2}\,\frac{g_{A,\ell}}{q^2 - m_Z^2 + im_Z\Gamma_Z}\,\Pi_Z, \\ c_3 &= \frac{1}{2}\,\frac{g_{V,\ell}}{q^2 - m_Z^2 + im_Z\Gamma_Z}\,\widetilde{\Pi}_Z + \frac{Q_\ell}{q^2}\,\widetilde{\Pi}_\gamma, \\ c_4 &= -\frac{1}{2}\,\frac{g_{A,\ell}}{q^2 - m_Z^2 + im_Z\Gamma_Z}\,\widetilde{\Pi}_Z \end{aligned} \qquad \text{(A1)}$$

with

$$\Pi_Z = \frac{eg^3}{16\pi^2 m_W}\Big[a_f\,\frac{2g_{V,f}}{c_W^2}\,N_f\,Q_f\,A_f(\lambda'_f,\lambda_f) + A_W(\lambda'_W,\lambda_W)\Big], \qquad \text{(A2)}$$

$$\Pi_\gamma = \frac{e^3 g}{16\pi^2 m_W}\Big[a_f\,4Q_f^2\,N_f\,A_f(\lambda'_f,\lambda_f) + A_W(\lambda'_W,\lambda_W)\Big], \qquad \text{(A3)}$$

$$\widetilde{\Pi}_Z = \frac{eg^3}{16\pi^2 m_W}\,b_f\,\frac{2g_{V,f}}{c_W^2}\,N_f\,Q_f\,I_2(\lambda'_f,\lambda_f), \qquad \text{(A4)}$$

$$\widetilde{\Pi}_\gamma = \frac{e^3 g}{16\pi^2 m_W}\,b_f\,4Q_f^2\,N_f\,I_2(\lambda'_f,\lambda_f). \qquad \text{(A5)}$$

Here, Γ_Z is the total decay width of the Z boson, $c_W \equiv \cos\theta_W$, where θ_W is the weak angle, $g = 2m_W(\sqrt{2}G_F)^{1/2}$, Q_f is the charge of the fermion in units of e, $g_{V,f} = t_{3L,f} - 2Q_f s_W^2$ ($g_{A,f} = t_{3L,f}$) is the $Zf\bar{f}$ vector coupling (axial-vector one), where $t_{3L,f}$ is a projection of the weak isospin.

The sum over all leptons and quarks in (A2)–(A5) is implied.

The loop integrals for fermions, $A_f(\lambda'_f,\lambda_f)$, and W bosons, $A_W(\lambda'_W,\lambda_W)$, are expressed via the loop functions $I_1(\lambda',\lambda)$ and $I_2(\lambda',\lambda)$ introduced in [23] and given explicitly in [12].

The arguments of these loop functions are

$$\lambda_{f,W} \equiv 4m_{f,W}^2/q^2, \quad \lambda'_{f,W} \equiv \lambda_{f,W}|_{q^2=m_h^2}. \qquad \text{(A6)}$$

Further, the coefficients in Eq. (9) are defined as follows:

$$\begin{aligned} A &= \frac{16}{(1-\beta_\ell^2 z^2)^2(m_h^2-q^2)^2}\Big[(m_h^4+q^4- \\ &- 8m_\ell^2 q^2)(1-\beta_\ell^2 z^2) + 32m_\ell^4 - 8m_h^2 m_\ell^2\Big], \\ \widetilde{A} &= \frac{16}{(1-\beta_\ell^2 z^2)^2(m_h^2-q^2)^2}\Big[(m_h^4+q^4)\times \\ &\times(1-\beta_\ell^2 z^2) - 8m_h^2 m_\ell^2\Big], \\ B &= -\frac{8m_\ell}{(1-\beta_\ell^2 z^2)}\Big[m_h^2 - q^2 + q^2\beta_\ell^2(1-z^2)\Big], \\ \widetilde{B} &= -\frac{8m_\ell}{(1-\beta_\ell^2 z^2)}\,(m_h^2-q^2)\,\beta_\ell\,z, \\ C &= -\frac{8m_\ell}{(1-\beta_\ell^2 z^2)}\,(m_h^2-q^2)\,\beta_\ell\,z, \\ \widetilde{C} &= \frac{8m_\ell}{(1-\beta_\ell^2 z^2)}(m_h^2-q^2), \\ D &= \frac{1}{2}(m_h^2-q^2)^2\Big[q^2(1+\beta_\ell^2 z^2) + 4m_\ell^2\Big], \\ E &= \frac{1}{2}(m_h^2-q^2)^2 q^2\,\beta_\ell^2(1+z^2), \\ F &= -(m_h^2-q^2)^2\,q^2\,\beta_\ell z \end{aligned} \qquad \text{(A7)}$$

with the notation $z \equiv \cos\theta$.

1. G. Aad *et al.* (ATLAS Collaboration), Observation of a new particle in the search for the Standard Model Higgs boson with the ATLAS detector at the LHC, *Phys. Lett. B* **716**, 1 (2012).
2. S. Chatrchyan *et al.* (CMS Collaboration), Observation of a new boson at a mass of 125 GeV with the CMS experiment at the LHC, *Phys. Lett. B* **716**, 30 (2012).
3. V. Khachatryan *et al.* (CMS Collaboration). Precise determination of the mass of the Higgs boson and tests of compatibility of its couplings with the standard model predictions using proton collisions at 7 and 8 TeV. *Eur. Phys. J. C* **75**, 212 (2015).
4. G. Aad *et al.* (ATLAS Collaboration). Measurements of the Higgs boson production and decay rates and coupling

strengths using *pp* collision data at $\sqrt{s} = 7$ and 8 TeV in the ATLAS experiment. *Eur. Phys. J. C* **76**, 6 (2016).
5. S. Chatrchyan *et al.* (CMS Collaboration). Study of the mass and spin-parity of the Higgs boson candidate via its decays to Z boson pairs. *Phys. Rev. Lett.* **110**, 081803 (2013).
6. G. Aad *et al.* (ATLAS Collaboration). Evidence for the spin-0 nature of the Higgs boson using ATLAS data. *Phys. Lett. B* **726**, 120 (2013).
7. V. Khachatryan *et al.* (CMS Collaboration). Constraints on the spin-parity and anomalous HVV couplings of the Higgs boson in proton collisions at 7 and 8 TeV. *Phys. Rev. D* **92**, 012004 (2015).
8. A.Yu. Korchin, V.A. Kovalchuk. Decay of the Higgs boson to $\tau^-\tau^+$ and non-Hermiticity of the Yukawa interaction. *Phys. Rev. D* **94**, no. 7, 076003 (2016).
9. C. Patrignani *et al.* (Particle Data Group). Review of Particle Physics. *Chin. Phys. C* **40**, 100001 (2016).
10. A.Yu. Korchin, V.A. Kovalchuk. Polarization effects in the Higgs boson decay to γZ and test of CP and CPT symmetries. *Phys. Rev. D* **88**, 036009 (2013).
11. A.Yu. Korchin, V.A. Kovalchuk. Higgs boson decay to γZ and test of CP and CPT symmetries. *Acta Phys. Polon. B* **44**, No. 11, 2121 (2013).
12. A.Yu. Korchin, V.A. Kovalchuk. Angular distribution and forward-backward asymmetry of the Higgs boson decay to photon and lepton pair. *Eur. Phys. J. C* **74**, 3141 (2014).
13. R.F. Streater, A.S. Wightman. *PCT, Spin and Statistics and All That* (Benjamin, 1964).
14. S. Heinemeyer, C. Mariotti, G. Passarino, R. Tanaka (Eds.). LHC Higgs Cross Section Working Group, Handbook of LHC Higgs Cross Sections:3. Higgs Properties, arXiv:1307.1347v1 [hep-ph].
15. A. Abbasabadi, D. Bowser-Chao, D.A. Dicus, W.W. Repko. Higgs photon associated production at $e\bar{e}$ colliders. *Phys. Rev. D* **52**, 3919 (1995).
16. A. Abbasabadi, D. Bowser-Chao, D.A. Dicus, W.W. Repko. Radiative Higgs boson decays H $\to$ fermion antifermion gamma. *Phys. Rev. D* **55**, 5647 (1997).
17. G.T. Bodwin, F. Petriello, S. Stoynev, M. Velasco. Higgs boson decays to quarkonia and the $H\bar{c}c$ coupling. *Phys. Rev. D* **88**, No. 5, 053003 (2013).
18. A.L. Kagan, G. Perez, F. Petriello, Y. Soreq, S. Stoynev, J. Zupan. An exclusive window onto Higgs Yukawa couplings. *Phys. Rev. Lett.* **114**, No. 10, 101802 (2015).
19. D.-N. Gao. A note on Higgs decays into Z boson and $J/\psi(\Upsilon)$. *Phys. Lett. B* **737**, 366 (2014).
20. B. Bhattacharya, A. Datta, D. London. Probing new physics in Higgs couplings to fermions using an angular analysis. *Phys. Lett. B* **736**, 421 (2014).
21. A. Kobakhidze, N. Liu, L. Wu, J. Yue. Implications of CP-violating top-Higgs couplings at LHC and Higgs factories. *Phys. Rev. D* **95**, No. 1, 015016 (2017).
22. S. Dittmaier, C. Mariotti, G. Passarino, R. Tanaka (Eds.). LHC Higgs Cross Section Working Group, Handbook of LHC Higgs Cross Sections: 1. Inclusive Observables, arXiv: 1101.0593v3 [hep-ph]
23. M. Spira. QCD Effects in Higgs physics. *Fortsch. Phys.* **46**, 203 (1998).

Received 24.04.17

В.А. Ковальчук, О.Ю. Корчин

РОЗПАД БОЗОНА ХІГГСА
НА ПАРУ ЛЕПТОНІВ ТА ФОТОН І МОЖЛИВА
НЕЕРМІТОВІСТЬ ВЗАЄМОДІЇ ЮКАВИ

Р е з ю м е

Досліджено народження лептонних пар у розпаді бозона Хіггса $h \to \ell^+\ell^-\gamma$. Акцент зроблено на структурі взаємодії бозона Хіггса з ферміонами. Ця взаємодія вибрана як суміш скалярної та псевдоскалярної частин, і, крім того, припускається, що вона може бути неермітовою. Вивчаються передбачення цієї моделі для спостережуваних у розпаді $h \to \ell^+\ell^-\gamma$ для e^+e^-, $\mu^+\mu^-$ і $\tau^+\tau^-$ пар. Розраховано диференціальну ширину розпаду і лептонну асиметрію "вперед-назад" як функції інваріантної маси ділептонів для декількох наборів констант $hf\bar{f}$ зв'язку. Вивчається вплив неермітовості $hf\bar{f}$ взаємодії на асиметрію вперед-назад, і підкреслюється великий вплив можливої неермітовості взаємодії бозона Хіггса з топ кварками на асиметрію вперед-назад для e^+e^- і $\mu^+\mu^-$ пар.